

# Carbon and amide detect backbone assignment methods of a novel repeat protein from the staphylocoagulase in *S. aureus*

Markus Voehler<sup>1</sup> · Maddur Appajiah Ashoka<sup>2</sup> · Jens Meiler<sup>1</sup> · Paul E. Bock<sup>2</sup>

Received: 9 March 2017 / Accepted: 5 August 2017 / Published online: 17 August 2017  
© Springer Science+Business Media B.V. 2017

**Abstract** The C-terminal repeat domain of staphylocoagulase that is secreted by the *S. aureus* is believed to play an important role interacting with fibrinogen and promotes blood clotting. To study this interaction by NMR, full assignment of each amide residue in the HSQC spectrum was required. Despite of the short sequence of the repeat construct, the HSQC spectrum contained a substantial amount of overlapped and exchange broadened resonances, indicating little secondary or tertiary structure. This caused severe problems while using the conventional, amide based NMR method for the backbone assignment. With the growing interest in small apparently disordered proteins, these issues are being faced more frequently. An alternative strategy to improve the backbone assignment capability involved carbon direct detection methods. Circumventing the amide proton detection offers a larger signal dispersion and more uniform signal intensity. For peptides with higher concentrations and in combination with the cold carbon channels of new cryoprobes, higher fields, and sufficiently long

relaxation times, the disadvantage of the lower sensitivity of the <sup>13</sup>C nucleus can be overcome. Another advantage of this method is the assignment of the proline backbone residues. Complete assignment with the carbon-detected strategy was achieved with a set of only two 3D, one 2D, and a HNCO measurement, which was necessary to translate the information to the HSQC spectrum.

**Keywords** Direct detect carbon · NMR · Backbone assignment · Bacterial endocarditis · Clotting · Staphylocoagulase · Intrinsically disordered protein (IDP)

## Context

A large fraction of the human genome encodes for proteins that lack persistent secondary or tertiary structure in isolation, so-called intrinsically disordered proteins (IDP) (Dyson and Wright 2004). However, these proteins do not violate the central dogma of structural biology—sequence determines structure, determines function—rather they can adopt a well-defined structure upon interaction with other partner biomolecules. That is, the secondary or tertiary structure is formed, often transiently, as a complex between the IDP and its partner molecule. IDPs play a vital role in our well-being and malfunction can lead to many diseases. Nuclear magnetic resonance (NMR) spectroscopy has evolved to a premier technique to study IDPs as it provides a toolbox to understand their dynamics and monitor structural changes upon interaction with their partners. Assignment of the signals, however, can be challenging as IDP spectra contain a substantial amount of overlapped and exchange broadened resonances. With a growing interest in the functionality and interaction of IDPs as part of regulatory network in the cell, finding ways to more completely assign them is crucial. In

Markus Voehler and Maddur Appajiah Ashoka have contributed equally.

**Electronic supplementary material** The online version of this article (doi:10.1007/s12104-017-9757-4) contains supplementary material, which is available to authorized users.

✉ Markus Voehler  
m.voehler@vanderbilt.edu

✉ Paul E. Bock  
paul.bock@vanderbilt.edu

<sup>1</sup> Department of Chemistry, Center for Structural Biology, Vanderbilt University, Nashville, TN 37232-8725, USA

<sup>2</sup> Department of Pathology, Microbiology, and Immunology, Vanderbilt University Medical Center, Nashville, TN 37232, USA

here, we turn to carbon direct detection methods to overcome these challenges and assign the backbone of a Novel Repeat Protein from the staphylocoagulase (SC) in *S. aureus*.

Blood clot formation is initiated by SC, secreted by *S. aureus*. Coagulase-positive *S. aureus* is a potent human pathogen that causes various diseases ranging from minor skin infections to life-threatening diseases such as severe pneumonia, meningitis, bone and joint infections, and infections of the heart. Each year more than 500,000 patients in American hospitals contract staphylococcal infections that could lead to acute bacterial endocarditis (ABE).

Bacterial endocarditis occurs by initial endothelium damage to heart valves due to turbulent blood flow, exposing the subendothelium and leading to deposition of platelets and fibrin (Fbn). The Fbn-platelet matrix deposited on damaged valves serves as a foci for adhering *S. aureus* bacteria circulating in the blood (Lowy 1998). The *S. aureus*-platelet interaction is mediated by fibrinogen (Fbg), fibronectin, thrombospondin, and microbial surface components recognizing adhesive matrix molecules (MSCRAMMs) like protein A and Fbg-binding clumping factor A (ClfA) which act as bridging molecules (Foster et al. 2014). The adhered bacteria further cause aggregation of platelets and enlargement of platelet-Fbn-bacteria vegetations due to Fbn formation by the SC·ProT\* complex on the valves, causing ABE (Lowy 1998).

SC is a bifunctional protein as depicted in Fig. 1. SC bypasses the clotting cascade by directly activating the zymogen prothrombin. The SC binds and activates prothrombin (ProT) non-proteolytically by inserting its N-terminal isoleucine (Ile)-valine (Val) residues into the isoleucine (Ile) 16 pocket of prothrombin (Friedrich et al. 2003). In the crystal structure of SC·ProT\* complex, ProT crystallizes as

SC·(pre)thrombin 2\* (Friedrich et al. 2003). SC·ProT\* active complex cleaves fibrinogen (Fbg) to form blood clots enlarging the vegetations. ABE caused by formation of *S. aureus* vegetations leads to 20–40% mortality in spite of antibiotic therapy. There is a gap in understanding the mechanism of Fbg interaction with the SC·ProT\* complex. We hypothesize that the C-terminal end of full length SC (1–660) in the SC·ProT\* complex is involved in Fbg binding. The effect of SC repeats on Fbg clotting by SC (1–660)·ProT\* complex is not known. The SC C-terminal repeats may play a role by enhancing the rate of clot formation.

Full length SC (1–660) from *S. aureus* Tager 104 Newman D2 strain contains 1 pseudo-repeat (PR), which is 32 residues in length, and 7 repeats (R1, R2, R3 ... R7), each 27 residues in length. Alignment of the pseudo-repeat and all 7 repeats shows a sequence homology of 30–40%, whereas alignment of the repeats alone shows a sequence homology of >80%. Our equilibrium binding studies showed that the pseudo-repeat along with a repeat unit 7, bind fibrinogen fragment D (Frag D) (unpublished). Our NMR studies have also shown that pseudo-repeat with repeat unit 7, PR-R7, binds to Frag D (unpublished).

## Methods and experiments

### Expression and purification of $^{15}\text{N}$ and $^{13}\text{C}$ PR-R7

The staphylocoagulase PR-R7 construct cDNA (coding for 75 residues) was cloned into a modified pET30b(+) vector (Novagen) as described (Friedrich et al. 2003). The C-terminal cysteine was introduced through QuikChange site-directed mutagenesis and confirmed by DNA sequencing.

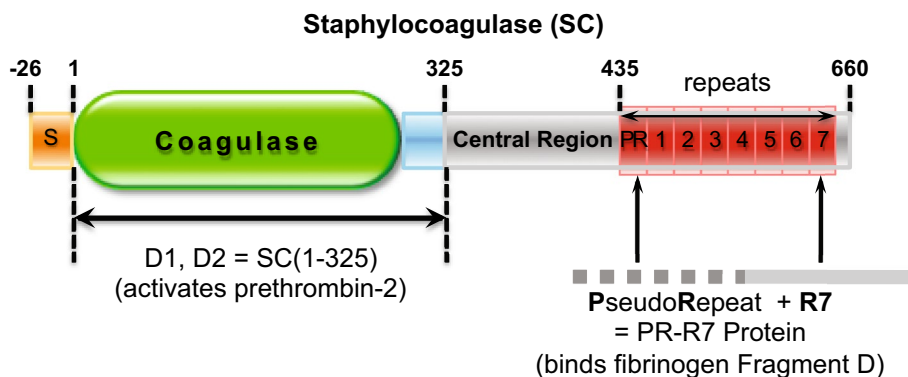


**Fig. 1** Biological context of the protein sample PR-R7 studied by NMR. Full length Staphylocoagulase (SC) consists of three major regions, the N-terminal D1 and D2 region, central region and C-terminal repeat region. The N-terminal region binds and activates prethrombin-2. A pseudo-repeat (PR) and seven homolog repeats

(R1.....R7) are located on the C-terminus of SC (1–660). The PR-R7 construct was chosen for these NMR studies because it was determined through equilibrium binding studies that Frag D binds to PR-R7 and its abundant expression in *E. coli* RS2 (DE3) pLysS

The PR-R7 construct containing a NH<sub>2</sub>-terminal His6-tag and tobacco etch virus cleavage site was transformed in to Rosetta 2 (DE3) pLysS *E. coli* cell line. The cells were grown in Bioexpress Cell Growth Media containing <sup>15</sup>N and <sup>13</sup>C isotopes, Cambridge Isotope Laboratories, Inc., Andover, MA, in the presence of 100 µg/ml kanamycin. The cells were grown at 37 °C until an O.D. reaches to 0.6 at 600 nm. The peptide was induced by adding 10 mg/ml lactose. After 4 h of induction, the culture was centrifuged at 5000×g for 30 min, and pellet was re-suspended in HEPES lysis buffer containing EDTA, PMSF, and D-Phe-Phe-Arg- and D-Phe-Pro-Arg-chloromethyl ketone inhibitors, in short FFR-CK and FPR-CK, respectively. The cells were lysed by three freeze–thaw cycles in liquid nitrogen and at 37 °C and the lysate was centrifuged at 39,200×g for 45 min. The protein in the inclusion bodies was purified by passing through nickel column (Friedrich et al. 2003). The His6-tag was removed as described (Panizzi et al. 2006) and the protein obtained was further purified by passing on C-15 reverse-phase high performance liquid chromatography (HPLC) column (5 µ × 4.6 mm × 150 mm, Beckman Coulter Inc.) and eluted with 0.1% trifluoro acetic acid (TFA) and 100% acetonitrile with 0.1% TFA. The HPLC fractions corresponding to the peak were pooled and lyophilized overnight. The lyophilized powder was re-suspended in 20 mM NaPO<sub>4</sub> and 150 mM NaCl, pH 7.0 and stored at –80 °C until use.

## NMR experiments

NMR experiments were performed at 298 K on Bruker AV-III 600.13 and 900.13 MHz spectrometers equipped with quadruple and triple resonance cryogenically cooled probes, a CPQCI and CPTCI, respectively. Two separate samples were prepared. The amide detected and the first set of carbon detect backbone experiments, were recorded in 350 µl of the re-suspended protein solution as described above, and were treated with FPR-CK and FFR-CK to a final concentration of 100 µM each. The solution was measured in a 4 mm NMR, inserted into a 5 mm NMR tube containing 200 µl D<sub>2</sub>O, as described in Voehler and Collier (Voehler et al. 2006). A second set of carbon direct detect measurements was measured with a 3 mm tube containing 200 µl of all of the above components plus 10 µl D<sub>2</sub>O for locking (Voehler et al. 2006). All experiments were run at 298 K and chemical shifts were referenced against the 4,4-dimethyl-4-silapentane-1-sulfonic acid (DSS) standard. NMR spectra were processed using Topspin 3.5 (Bruker BioSpin, Billerica, MA) and analyzed with NMRViewJ (One Moon Scientific, Inc., Westfield, NJ). Standard <sup>1</sup>H-<sup>15</sup>N HSQC experiments were used. Backbone resonance assignments were achieved by two distinctly different approaches, the traditional amide based method and two sets of carbon direct detect measurements. This allowed for a comparison of these three assignment methods and

their respective advantages/disadvantages. Specifics about each experimental condition can be found in Table 1 of the Supplementary Material. (1) Amide based assignments for <sup>1</sup>HN, <sup>15</sup>N, <sup>13</sup>C<sub>α</sub>, <sup>13</sup>C<sub>β</sub>, and <sup>13</sup>C' were made solving the connectivities derived from the six commonly employed 3D spectra HNCACB, CBCAcoNH, HNCA, HNcoCA, HNcaCO, and HNCO spectra (Sattler et al. 1999). (2) The carbon direct experiments CON, hnCOcaNCO, and hnCOcaNCO, as described by Pantoja-Uceda and Santoro (Pantoja-Uceda and Santoro 2013) provide a second set of backbone correlations. The magnetization pathway for the three dimensional experiments starts at the amide proton, and correlates the <sup>15</sup>N, <sup>13</sup>C<sub>α</sub>, and <sup>13</sup>C' of the protein backbone, meaning that the side-chain <sup>13</sup>C<sub>β</sub> atom was not part of the correlation network and all proline residue caused an interruption of the sequential assignment. (3) The same group published an improved version (Pantoja-Uceda and Santoro 2014) of the carbon direct detect method, which was used to measure the third set of backbone correlations. Here, the magnetization pathway starts at the α-proton compared to the amide one in the previous set, and therefore includes the proline residues so that a complete sequential walk without interruption was possible with this method. The chemical shift data has been deposited in the BMRB databank (<http://www.bmrwisc.edu>) and is retrievable under the Accession Number 27036.

## Assignment and data deposition

The complete assignment of the <sup>1</sup>H–<sup>15</sup>N HSQC spectrum provides information about the amides of a protein and their environment on an atomic level. It is therefore a valuable tool to follow protein interactions with high specificity for each amino acid using these short experiments. As indicated, this requires for all correlations in the HSQC spectrum to be assigned to their respective amino acid. This is achieved by a series of 3D experiments with complimenting information. The most commonly used set of experiments for globular proteins below 30 kDa are amide-detected experiments (Sattler et al. 1999).

Here, a set of the six commonly used backbone specific experiments were collected in a 4 mm NMR tube with 350 µl of about 1 mM sample at 600 MHz, using non-linear sampling methods to increase the resolution. Regardless of these efforts, 11 of the total 75 residues were initially not assignable. This did not include five proline residues that are present in the peptide. Such a large number of unassigned resonances was problematic for the future project, but is not uncommon when dealing with IDPs (Dyson and Wright 2004). Reasons for the large number of missing assignments in this study originate in the low or missing secondary structural content. This lead to minimal signal dispersion in the

amide proton dimension of  $8.2 \pm 0.27$  ppm, with a large fraction of overlapping peaks. Furthermore we found a number of weak resonances presumably due to exchange broadening.

Faced with these problems, other groups proposed approaches such as  $H\alpha$  detection (Mantylahti et al. 2011), separation of overlapping peaks through higher dimensionality (Bermel et al. 2012b), moving away from the amide detection to carbon, (Bermel et al. 2012a), and recently, nitrogen detection (Bermel et al. 2012a; Takeuchi et al. 2010). In an attempt to improve the number of assigned residues for the PR-R7 peptide, the carbon detect approaches from Pantoja-Uceda and Santoro (Pantoja-Uceda and Santoro 2013, 2014) were adopted. The main appeal of these methods was the sequential correlation of the carbonyl with their amide nitrogen atoms, both of which maintain a good dispersion even in unstructured proteins, and their relatively high sensitivity, as claimed by the authors. The magnetization pathway of the first set of experiments published started at the amide protons. This allowed for two possible pathways with observable magnetization, one including the auto-correlated and the other with only sequential peak detection. Analysis of the transfer function showed two maxima, one at a delay  $\lambda = 15$  ms, the other at  $\lambda = 28$  ms. Best performance was achieved at  $\lambda = 25$  ms, leaving the auto-correlation peaks practically unobservable. While this helps in reducing the peak crowding, it no longer differentiates the glycine resonances by their opposite phase appearance compared with the other signals, a small price to pay considering the distinct chemical shift for those residues. The 3D  $hNCOcaNCO$  experiment showed the  $^{13}C'(i)$ ,  $^{15}N(i)$ ,  $^{13}C'(i-1)$  peaks, and the  $^{15}N(i+1)$ ,  $^{15}N(i)$ ,  $^{13}C'(i-1)$  peaks were observed in the  $hNcocaNCO$  experiment. As pointed out by Santoro, analysis of the 3D spectra can be made by comparing the 2D— $^{15}N(i)$  planes of these two experiments with the 2D CON with peaks for  $^{15}N(i)$  and  $^{13}C'(i-1)$ . Correlations in the 3D  $^{15}N(i)$  planes lead to the next correlation in the CON spectrum with  $^{13}C'(i)$  and  $^{15}N(i+1)$  representing the succeeding amino acid in the sequence. While moving from the N-terminal towards the C-terminal is preferred, going the other direction is possible as well. Seven residue chains were identified, existing of continuous stretches of assigned residues. With five prolines, only six residue chains were expected. Upon closer examination the connection between Arg-25 and Asp-26 was identified containing unusually weak peaks in the  $hNCOcaNCO$  and  $hNcocaNCO$  experiments that was overlooked initially. Two assignment paths converged on one CON peak, which turned out to be a fully overlapped Tyr-9 and Tyr-68. Only one successive residue was identified, which had to be the Tyr-68 to the distinct shift of Gly-69, while Tyr-9 was followed by Pro-10 and therefore did not have a correlation. Thr-18 and Thr-59 were barely separated in the CON experiment, but showed very distinct shifts in the 3D experiments.

A second set of carbon direct detect experiments was acquired with a similarly concentrated protein sample (about 1 mM), but in a 3 mm NMR tube with about a third less volume than the previously used 4 mm tube. The experiments were based on the above principal as published by the same group a year later (Pantoja-Uceda and Santoro 2014). Improvements compared to the first set of experiments were implemented, while maintaining the good features from the previous set. These advances include (1) a reduced number of coherence transfer steps, yielding better sensitivity, (2) a practically unidirectional coherence transfer pathway, eliminating uninformative auto-correlation peaks, while maintaining the inverted phase of the glycine resonances to securely identify them. (3) And most importantly, the coherence transfer pathway in these experiments starts at the  $H\alpha$  proton and no longer at the amide proton, which means that proline residues no longer interrupt the sequential assignment and proline-rich polypeptides with multiple successive prolines can be assigned. The magnetization transfer pathway for the two complimentary 3D experiments is explained Pantoja-Uceda and Santoro (Pantoja-Uceda and Santoro 2014) and summarized here in short:  $hacoNcaNCO$ , where the observable peaks are  $^{13}C'(i-1)$ ,  $^{15}N(i)$ ,  $^{15}N(i+1)$ , and  $hacoConcaNCO$  with  $^{15}N(i-1)$ ,  $^{13}C'(i)$ ,  $^{15}N(i)$ , respectively. As in the previously described set, the  $^{15}N(i)$  planes of the 3D spectra are common to both 3D experiments. The resulting  $^{15}N(i+1)$  at the  $^{13}C'(i-1)$  chemical shift from the preceding CON correlation in the first experiment combined with the new  $^{13}C'(i)$  shift at the  $^{13}C'(i-1)$  chemical shift from the preceding CON correlation in the second 3D spectrum leads to the next residues CON correlation as described in Fig. 2. As before, assigning the sequence from the N- to the C-terminal is preferred, but moving the other way is possible too. Not surprisingly, the connection between Arg-25 and Asp-26 produced some weak peaks in these 3D spectra as they did in the other set of experiments, but since there were no breaks anticipated for the sequential assignment in this set, seeking for lower contour peaks quickly revealed those correlations. Asp-48 and Asn-49 also had weak correlation peaks in the 3D spectra, but they were stronger than the Arg-25 ones and continuation to the next residue was unambiguous. Pro-13 and Pro-45 were severely overlapped in all three spectra, but the resolution was sufficient to assign them individually after careful evaluation of each resonance. These proline peaks were only visible in this set of experiments; hence the problem was not observed in the previous set of experiments. This approach allowed full protein backbone assignments with only 4 days of acquiring the data, and about a day of data analysis. The acquisition for both sets of carbon detect experiments could have been shortened substantially, more along the 1 day per experiment as

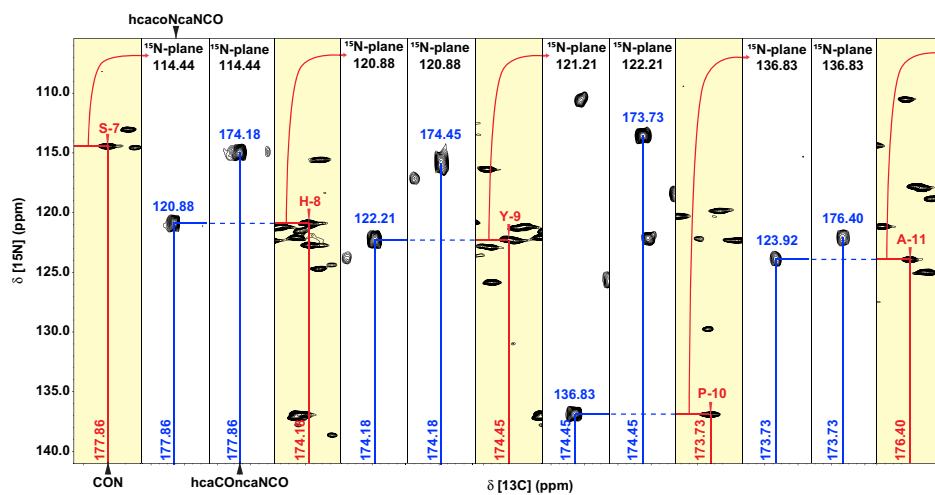


**Fig. 2** Assignment strategy for carbon direct detect experiments of PR-R7. All spectra were acquired at about 1 mM sample concentration, 3 mm tube, 298 K on a Bruker AV-III 900 MHz spectrometer with CPTCI probe. As an example, the assignment for residues S7–A11 of PR-R7 is shown here. The bases of the sequential backbone assignment for the carbon direct detect experiments is the CON spectrum (*yellow background*). From any correlation in the CON spectrum, the succeeding residue is found by searching the pair of planes at the  $^{15}\text{N}$ -chemical shift of that residue in the CON spectra with either the  $^{15}\text{N}$ ,  $^{13}\text{C}$ -plane in the 3D hcaONcaNCO spectrum, or the

$^{13}\text{C}$ ,  $^{13}\text{C}$ -plane in the 3D hcaCONcaNCO spectrum and their respective  $^{13}\text{C}$  chemical shift from the same residue in the CON spectrum. The *x*-axis shows the carbonyl chemical shift of the peak as described for each strip,  $\pm 0.2$  ppm. The *y*-axis shows the full range of the nitrogen dimension as shown on the *left* for the CON and the hcaONcaNCO strips, while the full carbon range (171.2–182.2 ppm) is used for the hcaCONcaNCO strips (not displayed). Chemical shifts of the peaks in the 3D spectra are labeled on *top* of the peak for the *y*-axis and on the *vertical line* for the *x*-axis

suggested by Santoro. Compared to the traditional experiments, both carbon detect data were very clean and mostly unambiguous, leading to 100% assignment of the backbone amide nitrogen and carbonyl carbons, not counting the N-terminal serine nitrogen and C-terminal cysteine carbonyl. Translation of the data to assign the  $^{15}\text{N}$ – $^1\text{H}$  HSQC was straight forward using the HCNO experiment.

With these assignments in hand, the amide-detected data was re-examined. All 11 missing residues could now be identified. Knowing the nitrogen and carbon carbonyl chemical shift from the carbon detect experiments helped to (1) resolve six previously missing assignments, Glu-2, Thr-3, Tyr-24, Tyr-34, Arg-44, and Val-72. These residues were in areas of the spectrum with heavy overlap and therefore difficult to assign. (2) Weak peaks could now be unambiguously assigned for His-8, Asn-16, Asn-54, His-61, Ala-62, and Ser-70 by examining lower contour levels in the 3D spectra. (3) Tyr-9 was initially not found due to its position in the sequence between Pro-10 that did not provide any correlations and His-8, which could not be assigned due to its weak peak. Based on the carbon direct detect data the HNCO peak was identified, but its close proximity to Glu-2 still left multiple assignment options open, which had to be carefully evaluated and assigned. Just reconciling the assignment for the amide-based experiments was more time-consuming than the data collection and analysis of the second carbon direct detection

experiment set, which is a strong argument for using that method on similar systems.

Final Backbone assignment for this protein was 100% of C', N (including proline), and 99% for  $\text{C}_\alpha$  and  $\text{C}_\beta$  (Ser-1 $\text{C}_\beta$  and His-8 $\text{C}_\alpha$  remain missing), as shown in Fig. 3. Side-chain proton and carbon atoms were assigned through the amide detected TOCSY experiments (Sattler et al. 1999).

Secondary structure prediction with Talos+ confirmed the total absence of either  $\alpha$ -helical or  $\beta$ -sheet structural features throughout the entire protein. This result was anticipated from the very limited amide proton dispersion and resonance overlap for many residues. Only residues Asp-26, Gly-37, Thr-60, His-61, Ala62, Asp-63 indicated a minimal propensity for secondary structure based on their chemical shift. The first two residues were not sequential and therefore not contributing to any secondary structural element. Even for the continuous residues His-61 to Asp-63, no secondary structure element was predicted. Asp-36 was the ambiguous residue in the Talos+ analysis and all others were deemed dynamic, e.g. non-structured.

In conclusion, the carbon direct detect backbone experiments, as described by Santoro, work very well for these short proteins with little to no structure. Cryogenically cooled probes with a cold carbon channel make these experiments feasible for protein concentrations at about 0.5–1 mM with measurement times of about a day. Compared to the amide detect experiments, this method provides easy

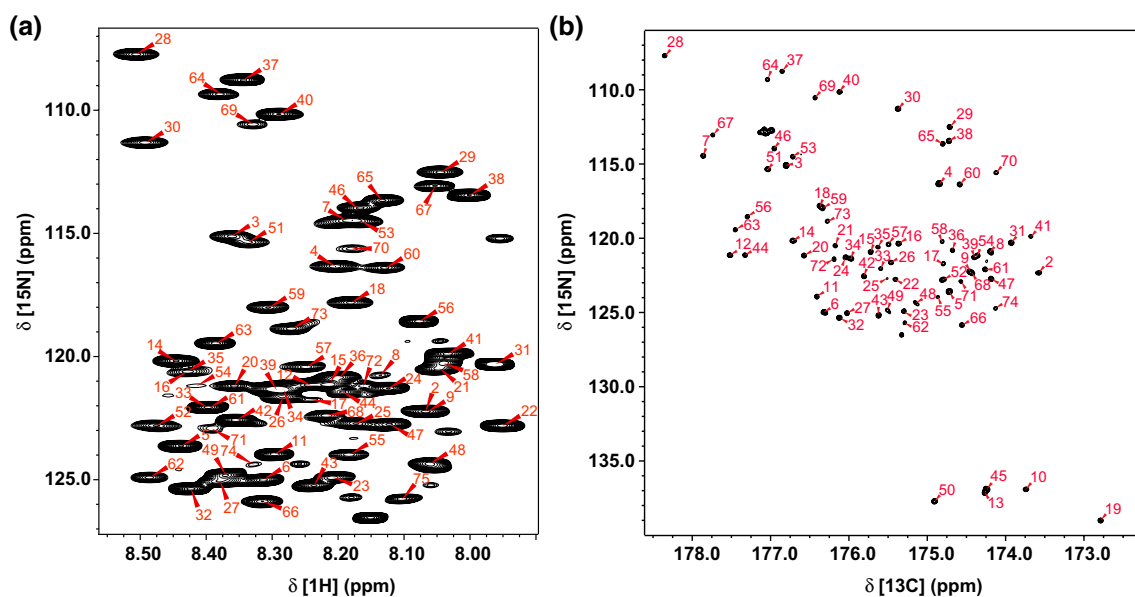


**Fig. 3** Assigned HSQC and CON NMR spectra in 20 mM NaPO<sub>4</sub>, 150 mM NaCl, 100 μM FFR-CK, and FPR-CK, pH 7.0. Data was collected at 298 K on a Bruker AV-III 900 MHz spectrometer with CPTCI probe. **a** The <sup>1</sup>H, <sup>15</sup>N-HSQC spectrum and assignments of the SC C-terminal repeat construct, PR-R7. **b** The carbon direct detect

CON spectrum with full assignment of all residues. The HSQC spectrum was fully assigned with the standard amide detected backbone experiments and further refined with the help of the carbon direct detect measurements as indicated in the text

interpretable spectra with few distinct peaks in each plane, allowing for quick and unambiguous assignments for most, if not all, residues. The simplicity of these spectra makes them also prime candidates for automated assignments. Translation from the C', N-assignment to the N-H amides peaks in the HSQC spectrum is carried out with the very sensitive HNCO spectrum. Although, the vast majority of the C' and N resonances are assignable this way, translation to the HSQC spectrum might still pose the problem of some residue overlap or weak resonances due to exchange broadening, as observed in this protein. Nonetheless, knowing the origin of these challenging HSQC peaks either as representation of multiple residues or exchange broadened peaks might still give some clues when studying protein interactions. If an overlapping resonance shifts, there is a good possibility that some of these peaks separate upon interaction with their titration partner and deliver the necessary information. The context might reveal, which of the two residues was affected. Weak peaks on the other hand provide limited information, but their appearance might strengthen upon binding. Since these peaks show up clearly in the carbon direct detect experiments, one might consider an interaction study using the CON experiment instead of the HSQC. The effect on the amide nitrogen will be the same, but the more sensitive amide proton will be missing and replaced with a better shielded carbonyl. While this experiment requires a double labeled sample, it might still be well worth the effort, depending on the importance of the interaction in question.

**Acknowledgements** We thank the group of J. Santoro for graciously providing the Bruker pulse programs for the carbon detect 3D experiments. This work was supported by US NIH Grants R01 HL071544 to PEB from the National, Heart, Lung and Blood Institute. The NMR instrumentation used in this work was supported by NIH S10 RR026677 and NSF DBI-0922862.

## References

- Bermel W, Bertini I, Chill J, Felli IC, Haba N, Kumar MVV, Pierattelli R (2012a) Exclusively heteronuclear C-13-detected amino-acid-selective NMR experiments for the study of intrinsically disordered proteins (IDPs). *ChemBiochem* 13:2425–2432. doi:[10.1002/cbic.201200447](https://doi.org/10.1002/cbic.201200447)
- Bermel W et al (2012b) Speeding up sequence specific assignment of IDPs. *J Biomol NMR* 53:293–301. doi:[10.1007/s10858-012-9639-0](https://doi.org/10.1007/s10858-012-9639-0)
- Dyson HJ, Wright PE (2004) Unfolded proteins and protein folding studied by NMR. *Chem Rev* 104:3607–3622. doi:[10.1021/cr030403s](https://doi.org/10.1021/cr030403s)
- Foster TJ, Geoghegan JA, Ganesh VK, Hook M (2014) Adhesion, invasion and evasion: the many functions of the surface proteins of *Staphylococcus aureus*. *Nat Rev Microbiol* 12:49–62. doi:[10.1038/nrmicro3161](https://doi.org/10.1038/nrmicro3161)
- Friedrich R et al (2003) Staphylocoagulase is a prototype for the mechanism of cofactor-induced zymogen activation. *Nature* 425:535–539. doi:[10.1038/nature01962](https://doi.org/10.1038/nature01962)
- Lowy FD (1998) *Staphylococcus aureus* infections. *N Engl J Med* 339:520–532. doi:[10.1056/NEJM199808203390806](https://doi.org/10.1056/NEJM199808203390806)
- Mantylähti S, Hellman M, Permi P (2011) Extension of the HA-detection based approach: (HCA)CON(CA)H and (HCA)NCO(CA)H experiments for the main-chain assignment of intrinsically

- disordered proteins. *J Biomol NMR* 49:99–109. doi:[10.1007/s10858-011-9470-z](https://doi.org/10.1007/s10858-011-9470-z)
- Panizzi P, Boxrud PD, Verhamme IM, Bock PE (2006) Binding of the COOH-terminal lysine residue of streptokinase to plasmin(ogen) kringles enhances formation of the streptokinase center dot plasmin(ogen) catalytic complexes. *J Biol Chem* 281:26774–26778. doi:[10.1074/jbc.C600171200](https://doi.org/10.1074/jbc.C600171200)
- Pantoja-Uceda D, Santoro J (2013) Direct correlation of consecutive C'-N groups in proteins: a method for the assignment of intrinsically disordered proteins. *J Biomol NMR* 57:57–63. doi:[10.1007/s10858-013-9765-3](https://doi.org/10.1007/s10858-013-9765-3)
- Pantoja-Uceda D, Santoro J (2014) New 13 C-detected experiments for the assignment of intrinsically disordered proteins. *J Biomol NMR* 59:43–50. doi:[10.1007/s10858-014-9827-1](https://doi.org/10.1007/s10858-014-9827-1)
- Sattler M, Schleucher J, Griesinger C (1999) Heteronuclear multidimensional NMR experiments for the structure determination of proteins in solution employing pulsed field gradients *Progress in Nuclear. Magn Reson Spectrosc* 34:93–158. doi:[10.1016/S0079-6565\(98\)00025-9](https://doi.org/10.1016/S0079-6565(98)00025-9)
- Takeuchi K, Heffron G, Sun ZYJ, Frueh DP, Wagner G (2010) Nitrogen-detected CAN and CON experiments as alternative experiments for main chain NMR resonance assignments. *J Biomol NMR* 47:271–282. doi:[10.1007/s10858-010-9430-z](https://doi.org/10.1007/s10858-010-9430-z)
- Voehler MW, Collier G, Young JK, Stone MP, Germann MW (2006) Performance of cryogenic probes as a function of ionic strength and sample tube geometry. *J Magn Reson* 183:102–109. doi:[10.1016/j.jmr.2006.08.002](https://doi.org/10.1016/j.jmr.2006.08.002)